Current Biology 20, 1197–1202, July 13, 2010 ©2010 Elsevier Ltd All rights reserved DOI 10.1016/j.cub.2010.05.038

Report

Wood Cell-Wall Structure Requires Local 2D-Microtubule Disassembly by a Novel Plasma Membrane-Anchored Protein

Yoshihisa Oda,[1,*] Yuki Iida,[1] Yuki Kondo,[1] and Hiroo Fukuda[1,*]
[1]Department of Biological Sciences, Graduate School of Science, The University of Tokyo, 7-3-1 Hongo, Bunkyo-ku Tokyo 113-0033, Japan

Summary

Plant cells have evolved cortical microtubules, in a two-dimensional space beneath the plasma membrane [1, 2], that regulate patterning of cellulose deposition [3]. Although recent studies have revealed that several microtubule-associated proteins [4–8] facilitate self-organization of transverse cortical microtubules [9–11], it is still unknown how diverse patterns of cortical microtubules are organized in different xylem cells [12–17], which are the major components of wood. Using our newly established in vitro xylem cell differentiation system, we found that a novel microtubule end-tracking protein, *mi*crotubule *d*epletion *d*omain *1* (MIDD1), was anchored to distinct plasma membrane domains and promoted local microtubule disassembly, resulting in pits on xylem cell walls. The introduction of RNA interference for *MIDD1* resulted in the failure of local microtubule depletion and the formation of secondary walls without pits. Conversely, the overexpression of *MIDD1* reduced microtubule density. MIDD1 has two coiled-coil domains for the binding to microtubules and for the anchorage to plasma membrane domains, respectively. Combination of the two coils caused end tracking of microtubules during shrinkage and suppressed their rescue events. Our results indicate that MIDD1 integrates spatial information in the plasma membrane with cortical microtubule dynamics for determining xylem cell wall pattern.

Results and Discussion

Cortical Microtubules Are Locally Disassembled in Differentiating Xylem Cells

VND6 is a master transcription factor that induces metaxylem vessel formation [18]. We produced four stable *Arabidopsis* cell lines harboring *VND6-YFP* or *VND6* (eVND6 line) placed under the control of the XVE system [19], which allows conditional expression with estrogen. All cell lines showed similar induction of metaxylem-like cells by estrogen. Differentiation into xylem cells started 24 hr after cell cultures were supplied with estrogen, and 80% of cells had differentiated at 48 hr (Figures 1A–1C). The vessel cells that formed had pitted or scalariform secondary walls that were typical patterns of metaxylem vessels (see Figures S1A–S1A″ available online).

Cortical microtubules in differentiating cells were distributed extensively under the developing secondary walls; however, only a few microtubules occurred beneath the pits in the secondary wall (Figure 1D; Figures S1E–S1F″). Microtubule depolymerization with oryzalin caused secondary wall deposition over the entire cell without making pits (Figures S1C and S1C′). Microtubule stabilization by taxol also affected the cell wall patterns (Figures S1D and S1D′). In contrast, the organization of actin microfilaments was not associated with secondary wall patterns (Figures S1G–S1G″). These results clearly indicated that the formation of secondary wall pits was associated with cortical microtubules. Time-lapse observations revealed a gradual disappearance of cortical microtubules at the future sites of secondary wall pits (Figure 1E). The cortical microtubules in these microtubule-depleted domains were highly unstable, as shown by the lower frequency of rescue events and higher frequency of catastrophic events compared with interphase cortical microtubules (Figure 1F; Table S1; Movie S1).

MIDD1 Functions in the Local Disassembly of Cortical Microtubules

To understand the molecular basis of the local disassembly of cortical microtubules, we searched for one or more key factors involved in this disassembly process. We selected five cytoskeleton-related genes and three genes encoding coiled-coil proteins of unknown function that are preferentially upregulated during xylem vessel differentiation, based on microarray data from a previous study [18]. These eight genes were fused with *GFP* and introduced into cultured *Arabidopsis* cells. The colocalization of each gene product with cortical microtubules was then examined. A novel protein, MIDD1 (AT3G53350), colocalized with cortical microtubules in vivo (Figure 2A). Fluorescence recovery after photobleaching analysis revealed their dynamic association with microtubules (Figures S2B and S2B′). Recombinant MIDD1 directly bound to the microtubules in vitro (Figure S4C). *MIDD1* was specifically upregulated after the expression of *VND6* in the cultured cells (Figure S2A). Consistent with this, eFP browser [20] indicated that *MIDD1* was expressed in xylem cells in roots. The eFP browser also suggested that *MIDD1* may be expressed in some floral tissues, such as stamens, petals, and pollens, indicating their involvement in other cell differentiations. Interestingly, in *pMIDD1::MIDD1-GFP*-transformed xylem cells, MIDD1 preferentially colocalized with cortical microtubules located beneath the secondary wall pits, but not with microtubules located outside of the pits (Figures 2B–2D; Figures S2C–S2F‴; Movie S2). Such heterogeneous localization of MIDD1 was observed prior to the secondary cell wall development (Figure S2D). MIDD1-GFP was also predominantly localized in the pits of secondary walls in taxol-treated cells (Figures S2G and S2G′). *MIDD1* encoded a 396-amino-acid-long protein of unknown function that was composed almost entirely of two coiled-coil domains (K67–S124 and L158–S366) and contained no other recognizable catalytic or structural domains (Figures S4A and S4A′). To understand the function of MIDD1, we introduced *p35S::MIDD1-RNAi* into the *XVE-VND6* cultured cell line. *MIDD1-RNAi* suppressed *MIDD1* mRNA levels to 20% of that of control cells (Figure 2H). *MIDD1-RNAi* did not inhibit xylem cell differentiation (Figure 2F); however, it did inhibit the formation of xylem cells with pitted secondary walls (Figures 2E and 2G). This result demonstrates that MIDD1 is

*Correspondence: oda@biol.s.u-tokyo.ac.jp (Y.O.), fukuda@biol.s.u-tokyo.ac.jp (H.F.)

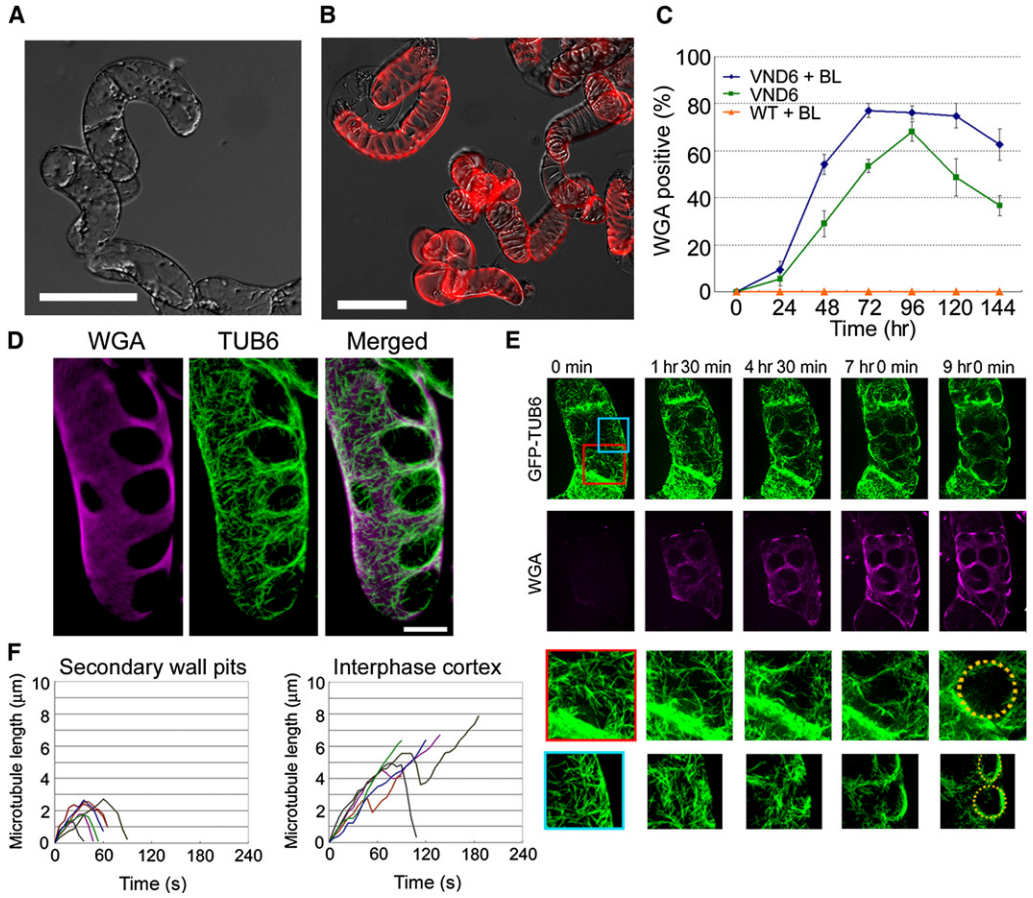

Figure 1. Local Disassembly of Cortical Microtubules during In Vitro Xylem Cell Differentiation

(A and B) Transgenic *Arabidopsis* suspension cells (eVND6 line) before (A) and after (B) addition of estrogen. Secondary cell walls (red) were stained with wheat germ agglutinin (WGA). Scale bars represent 20 μm.

(C) Time course of xylem cell differentiation. Estradiol was supplied at 0 hr of the graph. Values are means ± standard deviation (SD) of three experiments (n = 300 cells).

(D) Distribution of cortical microtubules (GFP-AtTUB6) and secondary cell walls stained with WGA Alexa Fluor 594. See also Figure S1. Scale bar represents 10 μm.

(E) Time-lapse observation of cortical microtubules and secondary walls in differentiating metaxylem-like cells. Note the gradual disappearance of cortical microtubules in the red and blue frames (GFP-TUB6, 0 hr). The regions in the red and blue frames are magnified and shown below.

(F) Life history plots of cortical microtubules in secondary wall pits and in the cortex of nondifferentiating interphase cells. Note that microtubules soon stop growing and begin shrinking in secondary wall pits, although microtubules continue to grow in nondifferentiating cells. See also Table S1 and Movie S1.

a key factor involved in the formation of secondary wall pits. Consistent with this effect, *MIDD1-RNAi* increased the number of xylem cells in which cortical microtubules were present in walls without pits (Figures 2I and 2J). Therefore, MIDD1 is likely to play a role in promoting cortical microtubule depolymerization at restricted domains, resulting in the formation of secondary wall pits. When MIDD1-GFP was conditionally expressed in nondifferentiating cells, MIDD1-GFP significantly reduced cortical microtubule density (Figures 2K and 2L), which suggests that MIDD1 promotes cortical microtubule depolymerization.

MIDD1 Accumulates at the Plus End of Shrinking Microtubules

To understand the molecular mechanisms underlying how MIDD1 is involved in cortical microtubule depolymerization, we investigated the dynamics of MIDD1-GFP along microtubules in developing xylem cells. Kymograph analysis indicated that MIDD1-GFP accumulated predominantly at the plus end of microtubules during shrinkage (Figures 3A–3D). Time-lapse observations of EB1-labeled microtubules supported the predominant localization of MIDD1 at the plus end of shrinking microtubules (Figure S3). The signal strength of MIDD1-GFP was the highest soon after catastrophic events (Figure 3E). These observations suggest that MIDD1 suppresses rescue events at the plus end of microtubules. Indeed, in cells expressing *MIDD1-GFP*, the rescue frequency of microtubules was remarkably reduced, whereas the growth rate or shrinkage rate was not affected (Table S1). Interestingly, a few immobile clusters of MIDD1-GFP remained along the trail of shrinkage (Figures 3A and 3B). Because RFP-TUB6 fluorescence was also observed with the clusters (Figure 3C), the clusters were considered to be complexes containing MIDD1 and microtubule fragments.

MIDD1 Is Anchored to Specific Domains of Plasma Membrane

To understand the domain function of MIDD1, we introduced truncated MIDD1 proteins fused with GFP into developing xylem cells. Truncated MIDD1 proteins lacking C-terminal

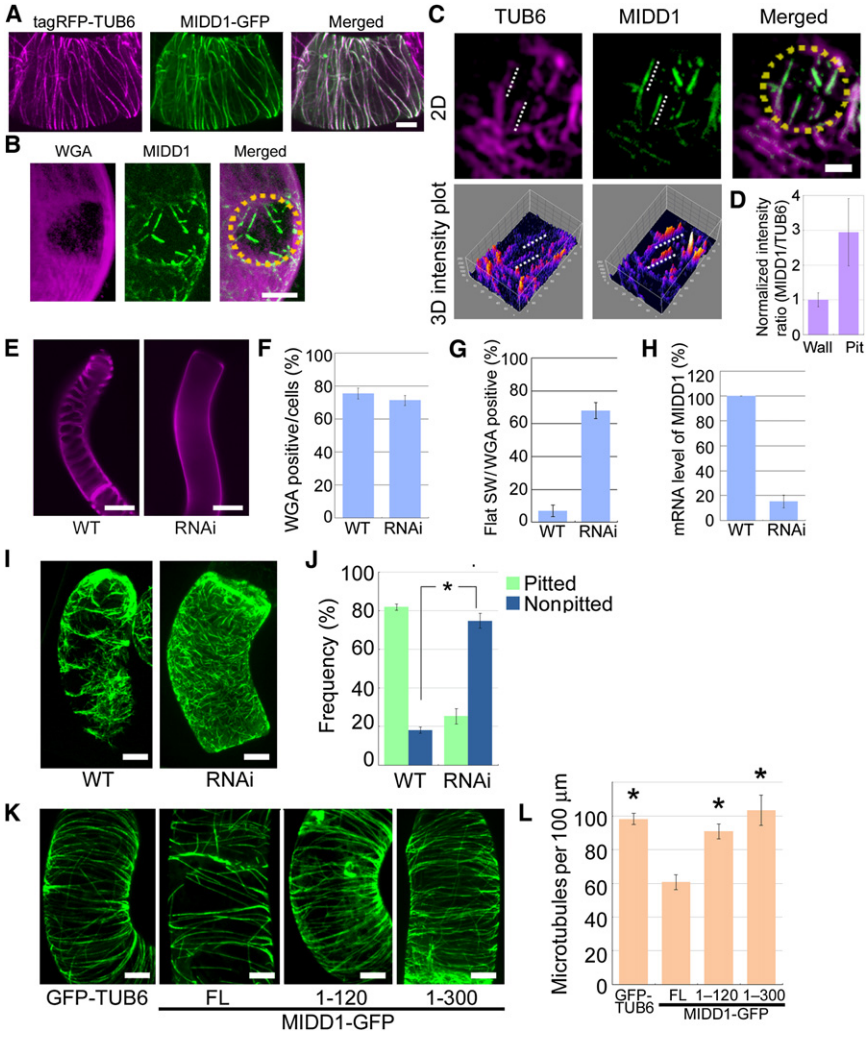

Figure 2. MIDD1 Functions in Depolymerization of Cortical Microtubules in Secondary Wall Pits

(A) Microtubules (*35S::tagRFP-TUB6*) and MIDD1 (*35S::MIDD1-GFP*) in the nondifferentiating cell.

(B) MIDD1 (*pMIDD1::MIDD1-GFP*) was localized preferentially in the secondary wall pit (yellow dotted circle).

(C) MIDD1 is colocalized with the microtubules in the pit (yellow dotted circle and white broken lines in the three-dimensional intensity plot), but not in areas outside of the pit.

(D) Intensity ratio of MIDD1-GFP and RFP-TUB6. Data are means ± SD of >25 microtubules from four cells, $p < 0.01$, t test. See also Figure S2 and Movie S2 for the localization of MIDD1.

(E–J) Effects of the *MIDD1-RNAi* construct when it was introduced to the eVND6 line.

(E) Secondary walls were stained with WGA.

(F) Percentage of cells with secondary cell walls. Values are means ± SD of three experiments (n > 300 cells).

(G) Percentage of cells with flat secondary walls without pits. Values are means ± SD of three experiments (n = 300 cells). $p < 0.01$, t test.

(H) mRNA level of *MIDD1* at 24 hr (n = 3). $p < 0.01$, t test.

(I) Cortical microtubule arrays (GFP-TUB6) at 24 hr.

(J) Percentage of cells with the pitted array of cortical microtubules at 24 hr. Values are means ± SD of four experiments (n > 50 cells). *$p < 0.01$, t test.

(K and L) Effects of conditional expression of full-length *MIDD1* gene (FL) and truncated *MIDD1* genes (1–300 and 1–120) for 24 hr on cortical microtubule density in nondifferentiating cells. Cortical microtubules were labeled with GFP-TUB6 or MIDD1-GFP. Values are means ± SD of three experiments (n = 40 cells). *$p < 0.01$ (analysis of variance [ANOVA] with Scheffe test versus FL). Only full-length MIDD1 (FL) decreased cortical microtubules. See also Table S1.

Scale bars represent 2 μm (B and C), 5 μm (A, I, and K), and 10 μm (E).

domains longer than 96 amino acids did not accumulate at the plus end of shrinking microtubules and were not retained as clusters on the trail of microtubule shrinkage (Figures 3F and 3G; Movie S3). The 120 amino acid N-terminal domain was enough to enable colocalization with cortical microtubules in vivo and in vitro (Figures S4B–S4D′); however, N-terminal domains shorter than 120 amino acids did not colocalize with microtubules (Figure S4B). This result indicates that the 96 amino acid C-terminal domain of MIDD1 is necessary for the localization on the plus ends of shrinking cortical microtubules and that the 120 amino acid N-terminal domain is necessary for colocalization with cortical microtubules. Indeed, although the 120 amino acid N-terminal domain of MIDD1 and MIDD1 proteins lacking C-terminal 96 amino acids colocalized with cortical microtubules (Figure 2K), they did not promote microtubule disassembly (Figure 2L; Table S1). Therefore, the binding of MIDD1 to the plus end of microtubules appears to be coupled with microtubule disassembly. Because truncated MIDD1 proteins lacking a C-terminal domain longer than 96 amino acids colocalized with cortical microtubules, but not specifically with microtubules inside of pits (Figures 4A and 4B; Figures S4D and S4D′; Movie S3), this suggests that a domain containing the C-terminal sequence may determine the pit-specific localization of MIDD1.

The 96 amino acid C-terminal domain is a part of the second coiled-coil domain (L158–S366) of MIDD1. Therefore, the subcellular localization of a truncated protein (amino acids 121–396) containing the second coiled-coil domain was examined. MIDD1$^{121–396}$-GFP did not colocalize with cortical microtubules as expected (Figure 4A). Instead, MIDD1$^{121–396}$-GFP accumulated along the cell cortex, in particular, just inside the thin wheat germ agglutinin-labeled cell wall in pits, suggesting that MIDD1$^{121–396}$-GFP localizes on the plasma membrane in contact with secondary wall pits (Figures 4C–4E). Such patched accumulation on the plasma membrane started in the early stages of differentiation, when secondary wall thickenings were not visible (Figures 4F–4H). These results indicate that MIDD1 is targeted to the plasma membrane of the pits through the second coiled-coil domain. MIDD1-GFP was still localized at distinct domains, even in the case in which cells were treated with oryzalin during differentiation (Figure S4E). This fact suggests that the targeting of MIDD1 into the plasma membrane domain is independent of the presence of cortical microtubules and secondary walls.

Here we have demonstrated that pits of the secondary walls in plant cells are formed by depolymerization of cortical microtubules beneath specific domains of the plasma membrane. MIDD1, a novel microtubule-associated protein, bridges the

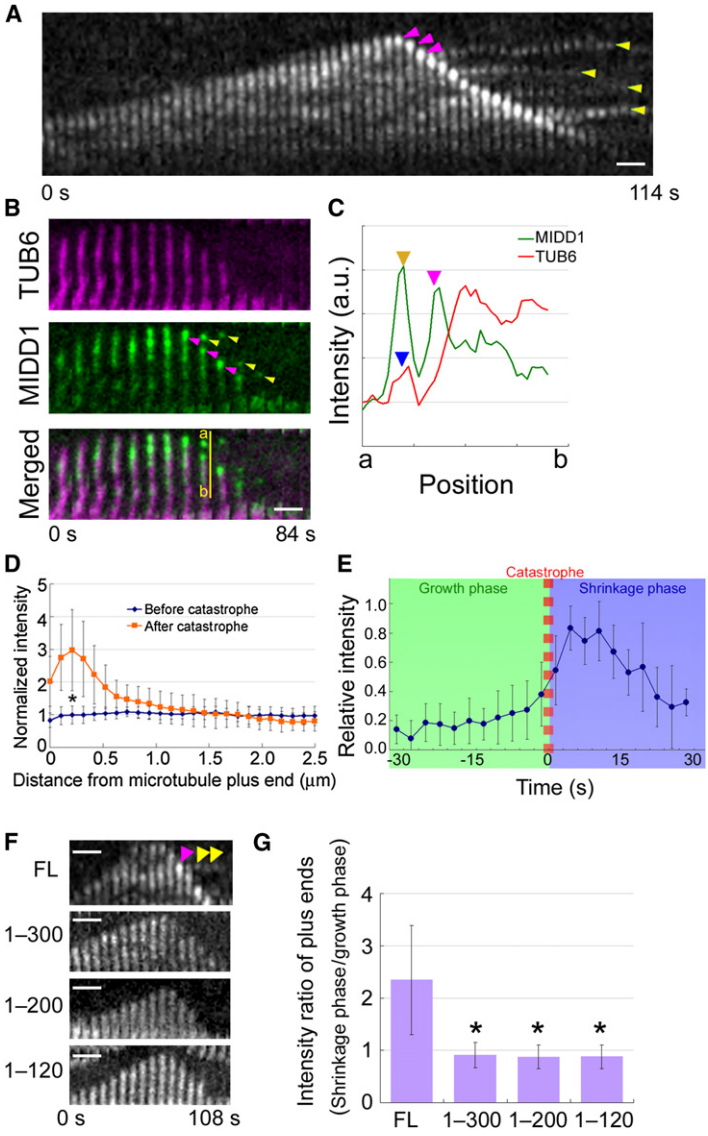

Figure 3. High Accumulation of MIDD1 at the Plus End of Shrinking Microtubules

(A) A kymograph of microtubules labeled with MIDD1-GFP in a secondary wall pit. Magenta arrowheads indicate strong signals of MIDD1-GFP during shrinkage. Yellow arrowheads indicate the remaining clusters of MIDD1-GFP. See also Figure S3 and Movie S2. Scale bar represents 1 μm.

(B) MIDD1-GFP accumulated at the plus end (magenta arrowheads) of microtubules (labeled with tagRFP-TUB6) during the shrinkage phase. Yellow arrowheads indicate clusters of MIDD1-GFP. Scale bar represents 1 μm.

(C) Intensity profile between positions a and b of (B) (merged). A weak peak (blue arrowhead) of the TUB6 signal was detected at the cluster of MIDD1 (yellow arrowhead).

(D) Intensity profile of MIDD1-GFP along microtubules. Values are means ± SD of 13 microtubules from four cells. *$p < 0.05$, t test.

(E) Intensity profile of MIDD1-GFP at the plus end of microtubules. Data are means ± SD of 15 microtubules from four cells.

(F) Kymographs of microtubules labeled with full-length MIDD1-GFP (FL) and truncated MIDD1-GFPs (1–300, 1–200, and 1–120) did not accumulate at the plus end of cortical microtubules (magenta arrowheads) or remain clustered (yellow arrowheads) during shrinkage. Scale bars represent 2 μm.

(G) Quantification of the intensity ratio of full-length MIDD1-GFP (FL) and truncated MIDD1-GFP proteins at the microtubule plus end. Data are means ± SD of >14 microtubules from >3 cells. *$p < 0.01$ (ANOVA with Scheffe test versus FL).

spatial information marked on the plasma membrane and cortical microtubule dynamics. Figures 4I–4K illustrate a possible model of cortical microtubule dynamics regulated by MIDD1. MIDD1 is recruited to plasma membrane domains (Figure 4I). When cortical microtubules grow into the cortical area beneath these domains, the microtubules are captured by MIDD1 (Figure 4J) and rescue events of cortical microtubules are prohibited, which results in local microtubule disassembly (Figure 4K). Recently, it was reported that vesicles that traffic cellulose synthase complexes are associated with microtubule plus ends during shrinkage [21]. Therefore, the active depolymerization of cortical microtubules at the distinct domains might cause elimination of cellulose synthase complexes from the domain, which effectively induces formation of secondary wall pits. MIDD1 is a member of the ICR/RIP family of proteins, which interacts with plant-specific Rac/Rho GTPases (ROPs) [22, 23]. It is known that some ROPs are localized at specific domains of the plasma membrane [24]. Therefore, MIDD1 might be recruited to the domains by interaction with ROPs and might function in depolymerization of cortical microtubules as an active ROP effector. In pollen tubes, ICR1/RIP1 associates with ROP1 and regulates polarized growth of pollen tubes [23]. ICRI/RIP1 forms oligomers [22], and the yeast Dam1 complex and kinesin-13 oligomerize to form a ring that is processively collected on the inside of curved protofilaments of microtubules during shrinkage in vitro [25–27]. *Drosophila* KLP59C, a member of the kinesin-13 family, inhibits the rescue of microtubules and is localized at the ends of shrinking microtubules [28]. Similarly, MIDD1 might be oligomerized to form rings around microtubules, enabling tracking of the ends and prohibiting rescue events, as shrinkage proceeds within the domain. As a result, MIDD1 mainly accumulates at the plus end of microtubules during shrinkage. MIDD1 might also preferentially bind to the curved microtubule protofilaments like kinesin-13s [29]. However, MIDD1 exists specifically in the plant kingdom and has an entirely different structure from kinesin-13. Thus, our study indicates that plant cells have developed unique subcellular regulatory machinery for the dynamics of two-dimensional microtubules at the plasma membrane.

Supplemental Information

Supplemental Information includes Supplemental Experimental Procedures, four figures, one table, and three movies and can be found with this article online at doi:10.1016/j.cub.2010.05.038.

Acknowledgments

We thank Masatoshi Yamaguchi of Nara Institute of Science and Technology (NAIST) and Taku Demura of RIKEN and NAIST for providing the inducible VND6 vectors, Nam-Hai Chua of the Rockefeller University for providing the pER8 vector, Ueli Grossniklaus of the University of Zurich for providing the pMDC7 vector, Tsuyoshi Nakagawa of Shimane University for providing the pGWB vectors, Jaideep Mathur of the University of Guelph for providing the GFP-EB1 fusion construct, Daisuke Miki of the University of California and Ko Shimamoto of NAIST for providing the pANDA35K vector, and Ken-ichi Wakabayashi and Ritsu Kamiya of

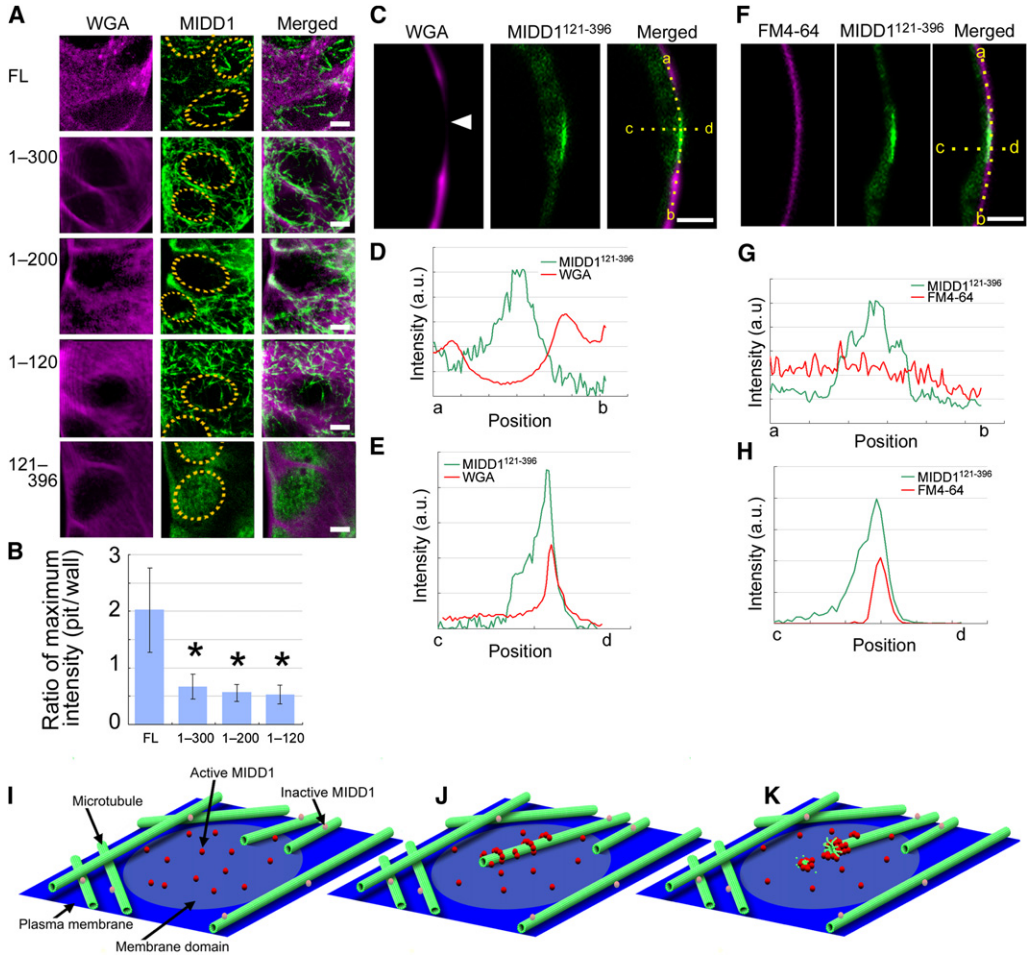

Figure 4. MIDD1 Anchored to Specific Domains of the Plasma Membrane

(A) Subcellular localization of truncated MIDD1-GFP proteins. Yellow dotted circles indicate secondary wall pits. Scale bars represent 1 μm.

(B) Quantification of the ratio of intensity of fluorescence from full-length MIDD1-GFP (FL) and truncated MIDD1-GFPs (1–300, 1–200, and 1–120) between the inside and outside of the pits. Data represent means ± SD of >14 pits from four cells, *$p < 0.01$ (ANOVA with Scheffe test versus FL). See also Figure S4 and Movie S3.

(C–E) Preferential localization of MIDD1$^{121–396}$-GFP beneath the pit (white arrowhead) of secondary walls. Scale bar represents 1 μm. Fluorescence intensities of WGA and MIDD1$^{121–396}$-GFP were quantified between positions a and b (D) and c and d (E) of (C).

(F–H) Preferential localization of MIDD1$^{121–396}$-GFP beneath a specific domain of the plasma membrane in immature xylem cells in which secondary wall formation was not visible. Scale bar represents 1 μm. Fluorescence intensities of FM4-64 and MIDD1$^{121–396}$-GFP were quantified between positions a and b (G) and c and d (H) of (F).

(I–K) A schematic model of local depolymerization of cortical microtubules caused by MIDD1. MIDD1 proteins anchored to specific domains of the plasma membrane (I) and captured growing cortical microtubules (J). The onset of shrinkage allowed MIDD1 proteins to accumulate at the plus end of the cortical microtubule, resulting in inhibition of rescue events for cortical microtubules (K).

The University of Tokyo and Takahiro Hamada of NAIST for technical advice about microtubule cosedimentation assays. This study was supported in part by the Japan Society for the Promotion of Science (Scientific Research grants 02718 to Y.O. and 20247003 to H.F.) and by Grants-in-Aid from the Ministry of Education, Science, Sports, and Culture of Japan (19060009 to H.F.).

Received: February 26, 2010
Revised: April 13, 2010
Accepted: May 3, 2010
Published online: June 17, 2010

References

1. Ehrhardt, D.W. (2008). Straighten up and fly right: Microtubule dynamics and organization of non-centrosomal arrays in higher plants. Curr. Opin. Cell Biol. *20*, 107–116.
2. Wasteneys, G.O., and Ambrose, J.C. (2009). Spatial organization of plant cortical microtubules: Close encounters of the 2D kind. Trends Cell Biol. *19*, 62–71.
3. Paredez, A.R., Somerville, C.R., and Ehrhardt, D.W. (2006). Visualization of cellulose synthase demonstrates functional association with microtubules. Science *312*, 1491–1495.
4. Ambrose, J.C., Shoji, T., Kotzer, A.M., Pighin, J.A., and Wasteneys, G.O. (2007). The Arabidopsis CLASP gene encodes a microtubule-associated protein involved in cell expansion and division. Plant Cell *19*, 2763–2775.
5. Furutani, I., Watanabe, Y., Prieto, R., Masukawa, M., Suzuki, K., Naoi, K., Thitamadee, S., Shikanai, T., and Hashimoto, T. (2000). The SPIRAL genes are required for directional control of cell elongation in Arabidopsis thaliana. Development *127*, 4443–4453.
6. Korolev, A.V., Buschmann, H., Doonan, J.H., and Lloyd, C.W. (2007). AtMAP70-5, a divergent member of the MAP70 family of microtubule-associated proteins, is required for anisotropic cell growth in Arabidopsis. J. Cell Sci. *120*, 2241–2247.

7. Sedbrook, J.C., and Kaloriti, D. (2008). Microtubules, MAPs and plant directional cell expansion. Trends Plant Sci. *13*, 303–310.
8. Whittington, A.T., Vugrek, O., Wei, K.J., Hasenbein, N.G., Sugimoto, K., Rashbrooke, M.C., and Wasteneys, G.O. (2001). MOR1 is essential for organizing cortical microtubules in plants. Nature *411*, 610–613.
9. Dixit, R., and Cyr, R. (2004). Encounters between dynamic cortical microtubules promote ordering of the cortical array through angle-dependent modifications of microtubule behavior. Plant Cell *16*, 3274–3284.
10. Murata, T., Sonobe, S., Baskin, T.I., Hyodo, S., Hasezawa, S., Nagata, T., Horio, T., and Hasebe, M. (2005). Microtubule-dependent microtubule nucleation based on recruitment of gamma-tubulin in higher plants. Nat. Cell Biol. *7*, 961–968.
11. Shaw, S.L., Kamyar, R., and Ehrhardt, D.W. (2003). Sustained microtubule treadmilling in Arabidopsis cortical arrays. Science *300*, 1715–1718.
12. Lloyd, C., and Chan, J. (2004). Microtubules and the shape of plants to come. Nat. Rev. Mol. Cell Biol. *5*, 13–22.
13. Mao, G., Buschmann, H., Doonan, J.H., and Lloyd, C.W. (2006). The role of MAP65-1 in microtubule bundling during Zinnia tracheary element formation. J. Cell Sci. *119*, 753–758.
14. Oda, Y., and Hasezawa, S. (2006). Cytoskeletal organization during xylem cell differentiation. J. Plant Res. *119*, 167–177.
15. Oda, Y., Mimura, T., and Hasezawa, S. (2005). Regulation of secondary cell wall development by cortical microtubules during tracheary element differentiation in Arabidopsis cell suspensions. Plant Physiol. *137*, 1027–1036.
16. Turner, S., Gallois, P., and Brown, D. (2007). Tracheary element differentiation. Annu. Rev. Plant Biol. *58*, 407–433.
17. Wightman, R., and Turner, S.R. (2008). The roles of the cytoskeleton during cellulose deposition at the secondary cell wall. Plant J. *54*, 794–805.
18. Kubo, M., Udagawa, M., Nishikubo, N., Horiguchi, G., Yamaguchi, M., Ito, J., Mimura, T., Fukuda, H., and Demura, T. (2005). Transcription switches for protoxylem and metaxylem vessel formation. Genes Dev. *19*, 1855–1860.
19. Zuo, J., Niu, Q.W., and Chua, N.H. (2000). Technical advance: An estrogen receptor-based transactivator XVE mediates highly inducible gene expression in transgenic plants. Plant J. *24*, 265–273.
20. Winter, D., Vinegar, B., Nahal, H., Ammar, R., Wilson, G.V., and Provart, N.J. (2007). An "Electronic Fluorescent Pictograph" browser for exploring and analyzing large-scale biological data sets. PLoS ONE *2*, e718.
21. Gutierrez, R., Lindeboom, J.J., Paredez, A.R., Emons, A.M.C., and Ehrhardt, D.W. (2009). Arabidopsis cortical microtubules position cellulose synthase delivery to the plasma membrane and interact with cellulose synthase trafficking compartments. Nat. Cell Biol. *11*, 797–806.
22. Lavy, M., Bloch, D., Hazak, O., Gutman, I., Poraty, L., Sorek, N., Sternberg, H., and Yalovsky, S. (2007). A Novel ROP/RAC effector links cell polarity, root-meristem maintenance, and vesicle trafficking. Curr. Biol. *17*, 947–952.
23. Li, S., Gu, Y., Yan, A., Lord, E., and Yang, Z.-B. (2008). RIP1 (ROP Interactive Partner 1)/ICR1 marks pollen germination sites and may act in the ROP1 pathway in the control of polarized pollen growth. Mol Plant *1*, 1021–1035.
24. Yang, Z. (2008). Cell polarity signaling in Arabidopsis. Annu. Rev. Cell Dev. Biol. *24*, 551–575.
25. Miranda, J.J.L., De Wulf, P., Sorger, P.K., and Harrison, S.C. (2005). The yeast DASH complex forms closed rings on microtubules. Nat. Struct. Mol. Biol. *12*, 138–143.
26. Tan, D., Asenjo, A.B., Mennella, V., Sharp, D.J., and Sosa, H. (2006). Kinesin-13s form rings around microtubules. J. Cell Biol. *175*, 25–31.
27. Westermann, S., Wang, H.-W., Avila-Sakar, A., Drubin, D.G., Nogales, E., and Barnes, G. (2006). The Dam1 kinetochore ring complex moves processively on depolymerizing microtubule ends. Nature *440*, 565–569.
28. Mennella, V., Rogers, G.C., Rogers, S.L., Buster, D.W., Vale, R.D., and Sharp, D.J. (2005). Functionally distinct kinesin-13 family members cooperate to regulate microtubule dynamics during interphase. Nat. Cell Biol. *7*, 235–245.
29. Mulder, A.M., Glavis-Bloom, A., Moores, C.A., Wagenbach, M., Carragher, B., Wordeman, L., and Milligan, R.A. (2009). A new model for binding of kinesin 13 to curved microtubule protofilaments. J. Cell Biol. *185*, 51–57.